

Promotion of the propane ODH reaction over supported V_2O_5/Al_2O_3 catalyst with secondary surface metal oxide additives

Brishti Mitra^a, Israel E. Wachs^b, Goutam Deo^{c,*}

^a Department of Chemical Engineering, University Institute of Engineering and Technology, CSJM University Kanpur, Kanpur 208 024, India

^b Operando Molecular Spectroscopy & Catalysis Lab., Chemical Engineering Department, Lehigh University, Bethlehem, PA 18015, USA

^c Department of Chemical Engineering, Indian Institute of Technology Kanpur, Kanpur 208 016, India

Received 23 January 2006; revised 23 March 2006; accepted 23 March 2006

Available online 24 April 2006

Abstract

Supported vanadia–alumina catalysts modified with chromium, molybdenum, and tungsten oxides were synthesized, characterized, and studied for their reactivity in the oxidative dehydrogenation (ODH) of methanol and propane. Raman and temperature-programmed reduction characterization studies revealed that only surface metal oxide species are present and that the modifiers are noninteracting in nature. Methanol ODH studies demonstrated that the modifiers cover the support acidic surface sites, are noninteracting in nature, and do not affect the surface vanadia redox product yield. The propane ODH reaction, however, revealed that the propylene yield increases when the surface MoO_x and WO_x are added to the supported vanadia–alumina catalysts. The surface MoO_x and WO_x modifiers are themselves relatively inert and appear to promote the propane adsorption step during the propane ODH reaction. The surface CrO_x modifier is more active than the surface vanadia sites for propane activation, but has a lower selectivity for propane ODH to propylene.

© 2006 Elsevier Inc. All rights reserved.

Keywords: Catalyst; Supported; Al_2O_3 ; V_2O_5 ; CrO_3 ; WO_3 ; MoO_3 ; Spectroscopy; Raman; H_2 -TPR; Oxidation; Oxidative dehydrogenation; ODH; CH_3OH ; C_3H_8 ; C_3H_6 ; Catalytic sites; Redox; Acidic

1. Introduction

The oxidative dehydrogenation (ODH) of propane to propylene has been extensively studied over supported vanadium oxide catalysts [1–11]. A major challenge in the commercial development of propane ODH catalytic technology is further improvement in the propylene yields, because significant carbon oxide byproducts are also formed. The main cause of the selectivity limitation arises from the conversion–selectivity relationship; an increase in conversion results in a decrease in propylene selectivity. One method to improve the yield of the desired product is to use surface metal oxide additives or modifiers that can further promote formation of the desired propylene product. The use of surface metal oxide modifiers possibly can tune the inverse conversion–selectivity relationship and result in enhanced propylene selectivity at higher propane con-

version. Based on a series reaction network for propane ODH to propylene and its subsequent oxidation to carbon oxides ($C_3 \rightarrow C_3^{\equiv} \rightarrow CO_x$), tuning of the inverse conversion–selectivity relationship can be achieved by increasing the k_1/k_2 ratio of the two reaction steps [12,13]. A triangular pseudo-first-order network taking the propane combustion step into consideration has also been used as a basis for understanding ways to increase propylene yield [14].

The desired action of surface metal oxide modifiers is alteration of the surface characteristics of the catalytic active sites to result in different k_1/k_2 ratios. The secondary surface metal oxide modifiers are proposed to be either interacting or noninteracting with the surface vanadia sites [15]. The interacting modifiers chemically coordinate with the surface vanadia species, affecting its catalytic properties, whereas the noninteracting modifiers coordinate with the oxide support and do not directly affect the catalytic properties of the surface vanadia species. Furthermore, metal oxides additives with relatively low oxidation states (e.g., Ni^{2+} , Co^{2+} , and Fe^{3+}) can strongly interact

* Corresponding author. Fax: +91 512 2590104.
E-mail address: goutam@iitk.ac.in (G. Deo).

with the surface defects of the Al_2O_3 support and form “surface spinel”-type species that are absorbed by the support subsurface region [16]. Recently, supported vanadia–alumina catalysts were modified by surface molybdenum (Mo) and chromium (Cr) oxides and investigated for propane ODH [17–19]. To the best of our knowledge, tungsten (W) oxide modification of supported vanadia–alumina catalysts has not been investigated in the open literature, although a tungsten-modified vanadia–titania catalyst has been considered [20]. Alkali [21–24], alkaline [25,26], manganese [23], and phosphorous [22] oxide additives to supported vanadia–alumina catalysts have also been studied for the propane ODH reaction.

In the present study, the metal oxide additives of Cr, Mo, and W were investigated to examine their effect on a supported vanadia–alumina catalyst for propane ODH. These elements are part of the group VIB of the periodic table and have varying redox ($\text{Cr} > \text{Mo} > \text{W}$) and acidic ($\text{W} > \text{Mo} > \text{Cr}$) characteristics [27,28]. The effect of these modifiers on the molecular structure and reducibility of the catalytic surface vanadia sites was studied. The chemical properties of the resulting modified supported $\text{V}_2\text{O}_5/\text{Al}_2\text{O}_3$ catalysts were probed with methanol and propane ODH catalytic reactions. Raman spectroscopy is commonly used for the characterization of surface metal oxide structures because of its ability to discriminate between different molecular structures based on their vibrational differences [29]. H_2 temperature-programmed reduction (TPR) studies have also been generally used for discriminating between different molecular structures due to its structure-dependent reduction behavior [30]. The methanol oxidation probe reaction has been shown to provide information about the different reactive sites present on the catalyst surface (redox, acidic, and basic) [31]. The relationships between the above structural and chemical characteristics and the targeted propane ODH reaction will provide additional fundamental insight into the influence of the various metal oxide modifiers on propane ODH over supported $\text{V}_2\text{O}_5/\text{Al}_2\text{O}_3$ catalysts.

2. Experimental

2.1. Catalyst preparation

The modified and unmodified $\text{V}_2\text{O}_5/\text{Al}_2\text{O}_3$ catalysts were prepared by the incipient wetness impregnation method. The

γ -alumina support was obtained from Condea (PURALOX, Sba 200). Seven catalyst samples were prepared for this study. The modifier, nomenclature, precursors used, and composition (wt% and atoms/ nm^2) of the different catalysts, along with the surface area and total metal oxide surface coverage, are given in Table 1. The Al_2O_3 support was initially pretreated with incipient volumes of oxalic acid solution; the details of the drying and calcination procedure are similar to the preparation of the catalysts and given elsewhere [9]. The incipient wetness impregnation of vanadium or co-impregnation of vanadium and modifier (chromium, molybdenum, and tungsten) ions from solution was then carried out on the pretreated support. The base $\text{V}_2\text{O}_5/\text{Al}_2\text{O}_3$ catalyst was prepared with less than half monolayer surface coverage. The molar ratio of modifier to vanadium was maintained at levels specified in Table 1. Each individual sample was thoroughly mixed and dried in air at room temperature overnight after impregnation, then at 383 K for 7 h and at 523 K for 6 h. The samples were finally calcined at 873 K for 6 h. To study the effect of chromia, molybdena, and tungsta modifiers on the properties of the supported $\text{V}_2\text{O}_5/\text{Al}_2\text{O}_3$ catalysts, vanadia-free supported $\text{Cr}_2\text{O}_3/\text{Al}_2\text{O}_5$, $\text{MoO}_3/\text{Al}_2\text{O}_5$, and $\text{WO}_3/\text{Al}_2\text{O}_5$ were also prepared by the incipient wetness impregnation method analogously to the preparation of the supported $\text{V}_2\text{O}_5/\text{Al}_2\text{O}_3$ catalysts. The amounts of chromium, molybdenum, and tungsten oxides used in these samples were the same as those used in the modified supported $\text{V}_2\text{O}_5/\text{Al}_2\text{O}_3$ catalysts.

2.2. Catalyst characterization

2.2.1. BET surface area

The surface areas of the samples were determined by a multipoint BET method using N_2 adsorption at 77 K. Degassing of the samples was achieved by heating in flowing helium at 423 K.

2.2.2. Raman spectroscopy

The catalysts were characterized by Raman spectroscopy under ambient and dehydrated conditions. The spectra were obtained using an ultraviolet (UV)–visible Raman spectrometer system (Horbia-Jobin Yvon LabRam-HR) with a confocal microscope, 2400/900 grooves/mm grating, and a notch filter. The samples were excited with a 532-nm Yag double-diode

Table 1
Specifications of the unmodified and modified supported vanadia–alumina catalysts

Modifier	Nomenclature	Precursor	V_2O_5 (%)	M_xO_y (%)	V^a (atoms/ nm^2)	$\text{M}^{a,b}$ (atoms/ nm^2)	Surface area (m^2/g)	Total surface coverage ^a
–	Al_2O_3	–	–	–	–	–	194	0
–	7WAl	$(\text{NH}_4)_6\text{H}_2\text{W}_{12}\text{O}_{14} \cdot 8\text{H}_2\text{O}$	–	7.0	–	1.0	199	0.22
–	5MoAl	$(\text{NH}_4)_6\text{Mo}_7\text{O}_{24} \cdot 4\text{H}_2\text{O}$	–	5.6	–	1.3	193	0.28
–	4CrAl	$\text{Cr}(\text{NO}_3)_3 \cdot 9\text{H}_2\text{O}$	–	4.0	–	1.7	200	0.42
–	7VAl	$\text{NH}_4\text{VO}_3 + \text{oxalic acid}$	7.3	–	2.7	–	159	0.37
WO_3	7W7VAl	$(\text{NH}_4)_6\text{H}_2\text{W}_{12}\text{O}_{14} \cdot 8\text{H}_2\text{O}$	6.8	6.6	2.7	1.0	–	0.59
MoO_3	5Mo7VAl	$(\text{NH}_4)_6\text{Mo}_7\text{O}_{24} \cdot 4\text{H}_2\text{O}$	6.9	5.2	2.7	1.3	153	0.64
Cr_2O_3	4Cr7VAl	$\text{Cr}(\text{NO}_3)_3 \cdot 9\text{H}_2\text{O}$	7.0	3.7	2.7	1.7	159	0.79

^a Based on pretreated Al_2O_3 surface area.

^b M = W, Mo and Cr.

pumped visible laser, and the spectral resolution was $\sim 2 \text{ cm}^{-1}$. The scattered photons were directed into a single monochromator (Jobin Yvon, LabRam-HR), and a UV-sensitive LN_2 CCD detector (Jobin Yvon CCD-3000V) was used to collect the scattered photons. The powdered samples were placed in an in situ cell (Linkam, TS-1500), which allows high-temperature treatments under different flowing gases. The samples were pretreated in flowing O_2/He at 673 K for 0.5 h before the Raman spectra of the dehydrated samples were obtained.

2.2.3. H_2 -TPR studies

H_2 -TPR studies were carried out on both the modified and unmodified supported $\text{V}_2\text{O}_5/\text{Al}_2\text{O}_3$ catalysts in an Altamira (AMI-100) system. A mixture of 10% H_2 -Ar at atmospheric pressure was used. Samples of $\sim 50 \text{ mg}$ were loaded into a quartz U-tube reactor and calcined in air at 773 K for 15 min. The samples were then cooled to 323 K, and dry argon was passed to remove the air used for calcination. The H_2 -TPR profiles were obtained by then passing the H_2 -Ar gas at a flow rate of $17 \mu\text{mol/s}$ and a heating rate of 10 K/min. The hydrogen consumption was monitored quantitatively using a thermal conductivity detector.

2.3. Reactivity studies

2.3.1. Methanol oxidation

The methanol oxidation reaction was carried out in an isothermal fixed-bed differential flow reactor operating at atmospheric pressure. A reactant gas mixture of $\text{CH}_3\text{OH}/\text{O}_2/\text{He}$ in a molar ratio of $\sim 7.1/14.4/78.8$ and total flow rate of $\sim 100 \text{ mL/min}$ was used for the reaction. The oxygen and helium mixture was sent through two independent mass flow controllers (Brooks) and bubbled through a methanol saturator cooled at 282.5 K. The cooling was achieved by flowing water from a cooler (Neslab RTE 112) through the saturator. The reactor was made of Pyrex glass (6 mm o.d.) and was held vertical with the gases flowing from top to bottom. The catalyst was supported on a layer of unreactive quartz glass wool. The catalyst amounts used were restricted to $\sim 25 \text{ mg}$, to maintain differential conditions. The reaction studies were carried out at 523 K. Each catalyst was pretreated at 623 K in a stream of flowing O_2 and He for 30 min before each run. The reactor was housed in a homemade furnace, and the temperature was controlled by a PID controller. The products were introduced into an on-line gas chromatograph (HP 5890 Series II) via a heated line and analyzed by a thermal conductivity detector (TCD) with a Carboxene-1000 packed column and a flame ionization detector (FID) with a CP-sil 5 CB capillary column connected in parallel.

2.3.2. ODH of propane

The ODH of propane was carried out at atmospheric pressure in an isothermal fixed-bed differential reactor with an i.d. of 6 mm. A catalyst amount of $\sim 50 \text{ mg}$ was used for each run. Net reducing conditions were maintained by using a reactant gas mixture with a $\text{C}_3\text{H}_8/\text{O}_2/\text{He}$ molar ratio of 9/3/38 and a total flow rate of $\sim 50 \text{ mL/min}$. The catalysts were pretreated in a

flowing O_2/He gas mixture at 753 K for 30 min before each run. Reaction temperatures were varied from 623 to 753 K for different catalysts. Product gases were analyzed using an on-line gas chromatograph (HP GC 6890 series) with both TCD and FID detectors. A Carboxene-1000 packed column and a Supelco capillary column (PQ1334-04) were used for the TCD and FID, respectively.

For both reaction studies, the activity, yield, and product selectivity were calculated based on the specific areas observed from the gas chromatography and the respective response factors. The reaction data were obtained at ~ 30 -min intervals for 2 h, during which no deactivation was observed. The methods used for calculating the activities, yields, and product selectivity are elaborated elsewhere [9,32].

3. Results and discussion

3.1. BET surface areas and metal oxide surface coverage

The surface areas of the seven catalysts along with the pretreated Al_2O_3 support are tabulated in Table 1. The surface area of the supported catalysts ranged from 153 to $200 \text{ m}^2/\text{g}$. Supporting small loadings of a single metal oxide component resulted in an insignificant decrease in surface area. The supporting of two metal oxide components, however, resulted in a noticeable decrease in surface area due to an increase in total mass of the supported metal oxides. A similar decrease in surface area with larger loadings of a single metal oxide species has been observed previously and is usually associated with the difference in the atomic weights among aluminum, vanadium, and the other modifiers and/or a decrease in the micropores. Furthermore, the X-ray diffraction patterns of the seven catalysts revealed only features of Al_2O_3 , suggesting that the support phase was not significantly affected during the synthesis steps.

The total surface metal oxide coverage was always maintained below monolayer coverage (see Table 1). Monolayer surface coverage values for the different metal oxides on Al_2O_3 were taken from previous studies [33] as VO_x , $\sim 7.3 \text{ V}/\text{nm}^2$; WO_x , $\sim 4.5 \text{ W}/\text{nm}^2$; MoO_x , $\sim 4.6 \text{ Mo}/\text{nm}^2$; and CrO_x , $\sim 4 \text{ Cr}/\text{nm}^2$. The vanadia loading was always maintained at 0.37 monolayer coverage, and the secondary metal oxide modifier loadings ranged from 0.2 to 0.4 monolayer coverage. In addition, the modifiers always constituted the minor component, and the surface VO_x was always the dominant metal oxide component in the catalysts.

3.2. In situ Raman spectroscopy

The Raman spectra of the dehydrated catalysts presented in Figs. 1a and 1b differ from those obtained under ambient conditions (not shown for brevity), reflecting the two-dimensional surface nature of these metal oxides. Comparing the Raman spectra of the dehydrated unmodified and modified supported $\text{V}_2\text{O}_5/\text{Al}_2\text{O}_3$ catalysts reveals that the vibration of the surface $\text{V}=\text{O}$ terminal bond, as well as the other VO_x vibrations, were

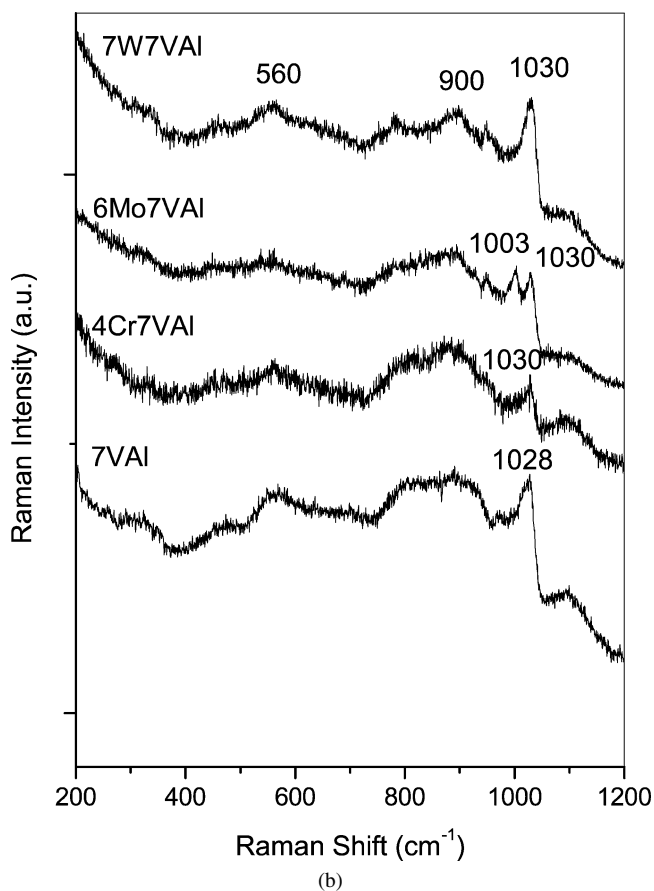
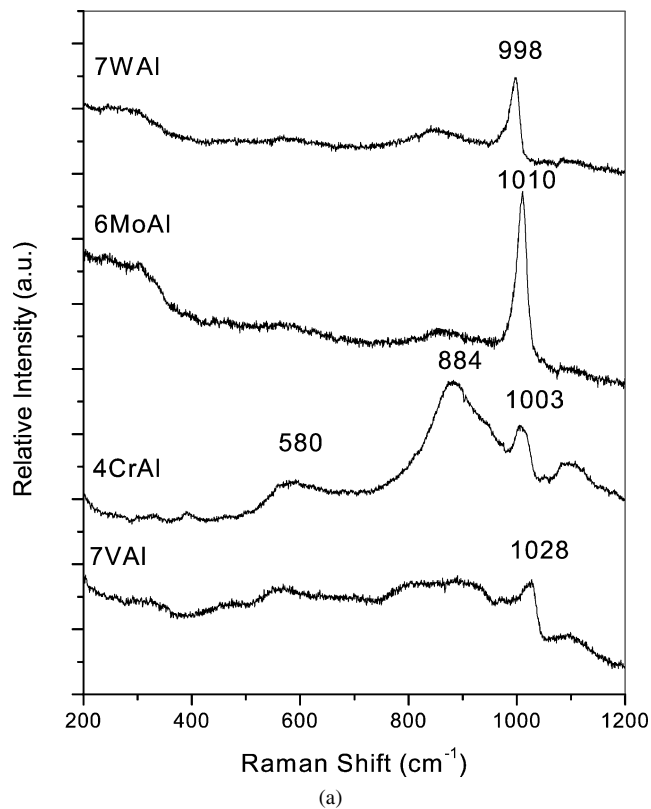


Fig. 1. (a) Raman spectra of dehydrated alumina supported metal oxide catalysts. (b) Raman spectra of dehydrated supported vanadia–alumina catalysts (unmodified and modified with secondary metal oxide additives).

essentially unaffected by the presence of the secondary surface metal oxide additives. The unmodified supported vanadia–alumina catalyst exhibited the V=O vibration at 1028 cm^{-1} and in the presence of the modifiers varied only slightly, from 1028 to 1030 cm^{-1} , within the experimental limitations of Raman spectroscopy. Small variations have also been observed with increasing surface vanadia (VO_x) loading, associated with minor changes in the V=O terminal bond strength due to polymerization of the surface VO_x with increasing surface coverage [34]. The vibrations of the terminal M=O bonds of the secondary surface metal oxide additives were observed at 1003 cm^{-1} for Cr=O, 1010 cm^{-1} for Mo=O, and 998 cm^{-1} for W=O. Strong Raman bands at 580 and 884 cm^{-1} have also been detected in the 4CrAl sample, associated with the polymeric surface chromate species [35]. Even with the increased total surface metal oxide coverage due to the addition of the surface modifiers, no distinct band associated with the polymeric surface vanadia species was observed as was previously reported in the Raman studies of Vuurman et al. [16]. For the modified samples, only surface molybdena species (MoO_x) gave rise to distinct Raman bands, reflecting that the relative Raman cross-section of the surface MoO_x species was the highest among the different secondary metal oxide modifiers used in the present study. Thus, in the presence of the surface metal oxide modifiers, no significant change in the molecular structure of the surface vanadium oxide species was observed for the samples used in this study. This suggests that the secondary metal oxide additives are functioning as noninteracting modifiers.

In addition, the absence of new Raman bands for the modified supported vanadia–alumina samples demonstrates the absence of crystalline bulk Cr–V–O, Mo–V–O, or W–V–O mixed oxide phases in these samples. The crystalline bulk Cr–V–O and Mo–V–O mixed oxides have been observed in supported metal oxide samples with more than a monolayer of total surface metal oxide coverage [18,19].

3.3. H_2 -TPR studies

The H_2 -TPR spectra of the alumina-supported metal oxide catalysts are presented in Fig. 2. The supported $\text{WO}_3/\text{Al}_2\text{O}_3$ catalyst was not found to reduce due to its well-known stabilization by the alumina support [36]. The hydrogen reduction temperatures, T_p , of the individual alumina-supported metal oxide catalysts increased as follows: CrO_x (640 K) < MoO_x (759 K) < VO_x (783 K) \ll WO_x . This trend indicates that the ease of oxygen removal by molecular H_2 from these surface metal oxide species varied in the following order: $\text{CrO}_x > \text{MoO}_x > \text{VO}_x \gg \text{WO}_x$. The addition of surface WO_x and MoO_x to the supported $\text{V}_2\text{O}_5/\text{Al}_2\text{O}_3$ catalysts had no or only a minor effect on the T_p reduction temperature of the surface VO_x species. But the addition of surface CrO_x to supported $\text{V}_2\text{O}_5/\text{Al}_2\text{O}_3$ introduced more easily reducible metal oxide sites, characteristic of the surface CrO_x species, and also slightly decreased the ease of oxygen removal by H_2 from the surface VO_x species (from 784 to 756 K). The latter effect may be related to some hydrogen spillover from the more easily reducible surface CrO_x species on Al_2O_3 . Thus, the H_2 -

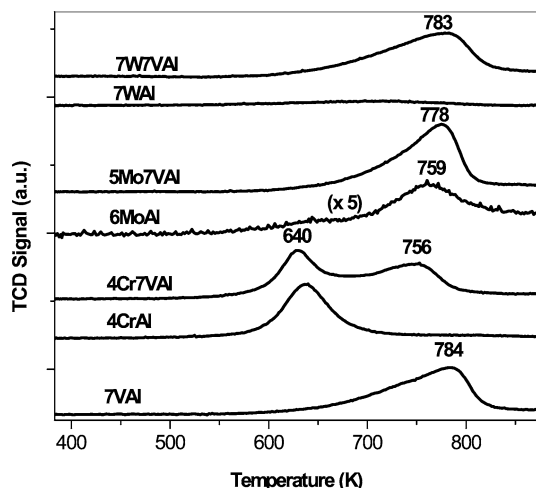


Fig. 2. H₂-TPR profiles of alumina supported metal oxide catalysts.

TPR results demonstrate that the ease of oxygen removal from the surface VO_x species on Al₂O₃ by molecular H₂ was either not affected or only mildly affected by the presence of group VI secondary surface metal oxide additives. This finding is in agreement with Raman findings discussed above, as well as earlier studies concluding that the group VI surface metal oxide species behave as noninteracting metal oxide additives [15].

No new reduction peak was observed for the modified alumina-supported vanadia catalysts, further confirming the absence of crystalline, bulk Cr–V–O, Mo–V–O, or W–V–O mixed oxide phases. Usually, the presence of new surface metal oxide molecular structures can be clearly discernible by Raman spectroscopy and H₂-TPR. For example, the presence of X-ray diffraction—amorphous α₁-VOPO₄ has been observed on Raman spectroscopy and H₂-TPR [13]. Consequently, no additional bulk mixed oxide phases were present in the modified supported vanadia–alumina catalysts.

3.4. CH₃OH oxidation

The catalytic activity, selectivity, and redox turnover frequency for the alumina-supported metal oxide catalysts and the pure alumina support are presented in Table 2. The pure Al₂O₃ support had no surface redox activity and was very active for the acid-catalyzed formation of dimethyl ether (DME). The acid-catalyzed formation of DME, however, was significantly suppressed with introduction of the surface metal oxides. Fig. 3 plots the DME yields over the different alumina-supported metal oxide catalysts versus the total surface metal oxide coverage. The DME yield continuously decreased with increasing surface metal oxide coverage independent of the specific surface metal oxide species. This indicates that DME formation originates from exposed alumina surface Lewis acid sites Al₂O₃, and these acidic sites are being titrated or covered by the surface metal oxide species. An increase in surface vanadia coverage also results in a continuous decrease in DME yield, because the surface vanadia sites progressively cover the exposed Al₂O₃ sites [32].

Table 2

Reactivity data for methanol oxidation over alumina supported metal oxide catalysts ($T = 523$ K; CH₃OH/O₂/He $\sim 7.1/14.4/78.8$; total flow rate ~ 100 sccm)

Catalyst	Activity (mol g _{cat} ⁻¹ h ⁻¹)	Selectivities (%)				Redox ^a turn- over frequency $\times 10^2$ (s ⁻¹)
		DME	HCHO	DMM	MF	
Al ₂ O ₃	0.531	100	0	0	0	0.00
7VAI	0.195	100	0	Trace	0	0.00
6MoAl	0.207	100	0	0	0	0.00
4CrAl	0.118	96	Trace	2	2	0.23 ^b
7VAI	0.185	66	28	4	2	2.22
7W7VAI	0.129	57	36	5	2	2.09
5Mo7VAI	0.144	57	38	4	1	2.24
4Cr7VAI	0.141	53	38	6	3	2.42

^a Corresponding to HCHO + DMM + MF formation per vanadium site, except 4CrAl.

^b Corresponding to HCHO, DMM and MF formation per chromium site.

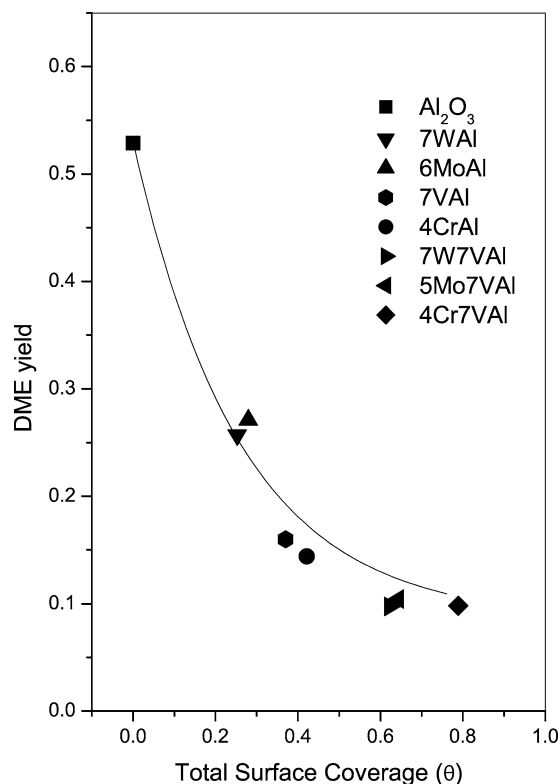


Fig. 3. Dimethyl ether (DME) yield during CH₃OH dehydration over alumina supported metal oxide catalysts versus total surface metal oxide coverage ($T = 523$ K; CH₃OH/O₂/He $\sim 7.1/14.4/78.8$; total flow rate ~ 100 sccm).

Analysis of the redox products of methanol oxidation, the sum of [formaldehyde (F) + methyl formate (MF) + dimethoxy methane (DMM)], over the alumina-supported vanadia catalysts reveals that the turnover frequency (TOF) of the redox products, given in Table 2, was not affected by the presence of secondary surface metal oxide additives. This suggests that the supported metal oxide additives are significantly less active than the surface vanadia species for the ODH of CH₃OH to HCHO. Similar results were previously found for the effect of noninteracting modifiers on V₂O₅/TiO₂ catalysts for methanol ODH to formaldehyde [15]. Thus, the ODH activity of the cat-

Table 3
Reactivity data for propane ODH over alumina supported metal oxide catalysts ($T = 653$ K; $C_3H_8/O_2/He = 9/3/38$; total flow rate = 50 sccm)

Catalyst	Activity $\times 10^2$ ($\text{mol g}_{\text{cat}}^{-1} \text{h}^{-1}$)	Selectivities (%)			Overall TOF ^a $\times 10^3$ (s^{-1})
		C_3H_6	CO	CO_2	
Al_2O_3	0.02	0	100	0	
7VAI	0.03	0	100	0	0.12
6MoAl	0.05	0	74	26	0.18
4CrAl	1.4	24	27	49	7.29
7VAI	1.1	72	17	11	4.27
7W7VAI	2.3	70	18	12	
5Mo7VAI	2.1	72	17	11	
4Cr7VAI	6.8	49	32	19	

^a Based on single component surface metal oxide species.

alytic active surface vanadia redox sites, as chemically probed by methanol oxidation, was not perturbed by the presence of secondary surface metal oxide additives.

3.5. Propane ODH

The propane ODH findings over the supported metal oxide catalysts are presented in Table 3. The alumina support showed no selective propane oxidation activity under the chosen reaction conditions. The alumina-supported tungsta and molybdena catalysts were also inactive for the selective propane ODH to propylene, and only CO_x byproducts were detected. The alumina-supported chromia and vanadia catalysts were significantly more active than the alumina-supported tungsta and molybdena catalysts, with an overall TOF about two orders of magnitude greater. The overall TOF for the surface CrO_x species was higher than that for the surface VO_x species, but the propylene selectivity trend was inverse to that for activity (72% for supported V_2O_5/Al_2O_3 vs. 24% for supported CrO_3/Al_2O_3).

The propane ODH to propylene over the supported V_2O_5/Al_2O_3 catalysts was significantly influenced by the presence of secondary surface metal oxide additives. Both surface WO_x and MoO_x are inactive for propane ODH, but their presence enhances the selective ODH of propane to propylene by increasing the activity by a factor of ~ 2 and maintaining the same selectivity. Adding surface CrO_x to supported V_2O_5/Al_2O_3 increased the activity by a factor of ~ 6 , but with an accompanying decrease in propylene selectivity from 72 to 49%. Nevertheless, the overall yield of propylene from propane ODH was enhanced significantly (see Fig. 4). The lower propylene selectivity for the 4Cr7VAI sample may be partly due to the higher conversion considered. The increase in overall propane ODH activity was larger than the sum of the individual surface metal oxide species, because both alumina-supported surface WO_x and MoO_x species are essentially inactive for propane ODH, but their addition significantly enhances propane ODH activity. Thus, the secondary group VI surface metal oxide additives promote the supported V_2O_5/Al_2O_3 catalysts for the propane ODH reaction and its selective formation of propylene.

Comparing the propane ODH and propylene selectivity values in Table 3 reveals that the supported 7W7VAI and 5Mo7VAI catalysts have similar selectivity to the supported 7VAI sample.

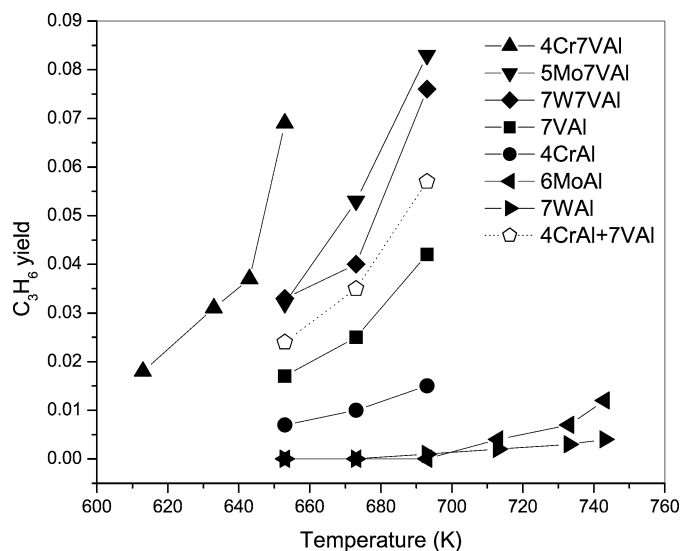


Fig. 4. Propylene yield during propane ODH over alumina supported metal oxide catalysts at different temperatures ($C_3H_8/O_2/He = 9/3/38$; total flow rate = 50 sccm). 4CrAl + 7VAI correspond to the cumulative C_3H_6 yields of 4CrAl and 7VAI. Cumulative C_3H_6 yields for 6MoAl + 7VAI and 7W7VAI + 7VAI overlap the C_3H_6 yields of 7VAI.

These catalysts' similar propylene selectivity suggests that exposed surface alumina sites play an insignificant role in the conversion of propylene to carbon oxides, because these catalysts have variable surface metal oxide coverage (see Table 1). This is consistent with the results of Fourier transform infrared spectroscopy studies on pure Al_2O_3 that found no propylene adsorption at 373 K [26]. The propylene selectivity of the 4Cr7VAI sample was between that of the 4CrAl and 7VAI catalysts, reflecting that both surface VO_x and CrO_x sites were active for propane ODH to propylene, with the latter being less selective.

The promotional effect of the secondary group VI surface metal oxide modifiers on supported V_2O_5/Al_2O_3 catalyst for propane ODH to propylene is further shown in Fig. 4, which plots the propylene yield versus the reaction temperature. The propylene yield increased with reaction temperature for all the catalysts, due primarily to the difference in activation energy between propylene and carbon oxide formation. The propylene yields of the modified supported vanadia–alumina catalysts were greater than those of the individual supported metal oxide catalysts at all temperatures. The propylene yield of the chromia modified vanadia–alumina catalyst was the greatest and larger than the combined yield of supported V_2O_5/Al_2O_3 and Cr_2O_3/Al_2O_3 catalysts, as also shown in Fig. 4. The yields for the tungsta- and molybdena-modified vanadia–alumina catalysts were similar, but greater than the propylene yields for the unmodified alumina–vanadia catalyst. The combined propylene yields of the $V_2O_5/Al_2O_3 + WO_3/Al_2O_3$ and $V_2O_5/Al_2O_3 + MoO_3/Al_2O_3$ catalysts were similar to the propylene yield of the supported V_2O_5/Al_2O_3 catalysts, because the supported WO_3/Al_2O_3 and MoO_3/Al_2O_3 catalysts are essentially inactive. Thus, the promotional effect of the secondary group VI metal oxide modifiers for the propane ODH reaction is not due to the presence of a new phase, a change in the strength of the redox centers, or a change in the exposed alumina sites.

To understand the promotional effect in terms of kinetic parameters, it is worthwhile to consider a simplified network for the propane oxidation reaction where propylene is the intermediate or primary product and the carbon oxides are the secondary or final products [9,12,13]. Based on this reaction model, the increase in propane oxidation activity in Table 3 can be seen to result from an increase in the rate constant for propylene formation, k_1 . No information about the variations in the rate constant for carbon oxide formation, k_2 , can be deduced from the present investigation, although recent kinetic parameter studies reveal that the value of k_2 is not significantly affected for the WO_x - and MoO_x -modified $\text{V}_2\text{O}_5/\text{Al}_2\text{O}_3$ catalysts. The rate constant k_1 contain the pre-exponential factor, k_{10} , and activation energy, E_1 . The apparent activation energy values for propylene formation are calculated based on the propylene yields as a function of reaction temperature. Such estimates of apparent activation energies are approximate, and additional experiments are needed for more reliable values. For the supported 7VAI, 7W7VAI, 5Mo7VAI, and 4Cr7VAI catalysts, the apparent activation energies for propylene formation are not very different: 85, 78, 90, and 81 kJ/mol, respectively. Consequently, the promotional effect of the secondary group VI surface metal oxide modifiers does not appear to reside in changes of the activation energy term for propane ODH to propylene.

The similarity of the propylene formation activation energies for the modified supported $\text{V}_2\text{O}_5/\text{Al}_2\text{O}_3$ catalysts suggests that the promotional effect is due to the increase in the pre-exponential k_{10} values. One of the major terms in the pre-exponential k_{10} value is the equilibrium adsorption constant. This suggests that the noninteracting and inactive secondary surface metal oxide additives, with the exception of the active surface CrO_x species, enhance the propane adsorption equilibrium constant over the supported $\text{V}_2\text{O}_5/\text{Al}_2\text{O}_3$ catalysts. This implies that propane is able to adsorb in a precursor state on the secondary surface metal oxide sites that can supply the weakly adsorbed propane to the catalytic active surface VO_x sites for activation to propylene. Consequently, the same propylene selectivity values are observed for the surface MoO_x and WO_x modified and unmodified supported $\text{V}_2\text{O}_5/\text{Al}_2\text{O}_3$ catalysts. For the CrO_x -modified supported $\text{V}_2\text{O}_5/\text{Al}_2\text{O}_3$ catalyst, the situation is more complex, because both the surface CrO_x and VO_x sites are active for propane activation to propylene, even though different selectivities are observed. The propane equilibrium adsorption constant is affected by both surface metal oxide sites, and the adsorbed propane is converted to propylene and further to carbon oxides, depending on the whether the activation occurs on the surface vanadia or chromia sites.

3.6. Molecular structure–activity/selectivity relationships

The alumina-supported VO_x and MO_x ($M = \text{Cr}, \text{Mo},$ and W) metal oxides used in this investigation are present exclusively as surface metal oxide species coordinated to the alumina support. The secondary group VI surface metal oxide modifiers behave as noninteracting additives because they do not

significantly alter the molecular structure of the surface VO_x species of the supported $\text{V}_2\text{O}_5/\text{Al}_2\text{O}_3$ catalysts. The noninteracting nature of these secondary surface metal oxide additives is further reflected in the almost unperturbed reduction characteristics of the alumina-supported surface VO_x species involving oxygen extraction by molecular H_2 during H_2 -TPR experiments. A similar conclusion is reached when the redox characteristics of the various supported $\text{V}_2\text{O}_5/\text{Al}_2\text{O}_3$ catalysts are chemically probed with methanol ODH to formaldehyde. The secondary surface metal oxide additives have almost no redox activity for methanol ODH, and the redox yield of the modified alumina-supported vanadia catalysts is essentially invariant to the presence of the secondary surface metal oxide additives (see Tables 2 and 3). However, the corresponding propylene yields during propane ODH are significantly enhanced by the presence of the surface metal oxide additives even though the surface MoO_x and WO_x additives are almost inactive for this reaction. Kinetic analysis of the propane ODH reaction over the supported $\text{V}_2\text{O}_5/\text{Al}_2\text{O}_3$ catalysts suggests that the origin of this enhancement resides in the kinetic pre-exponential factor that contains the adsorption equilibrium constant.

The model for the modified supported vanadia–alumina catalysts that accounts for the different reactivity trends of these catalysts for methanol and propane ODH reaction is shown in Fig. 5. Dissociative CH_3OH chemisorption readily proceeds on supported VO_x sites, and the adsorption process is not activated, with the rate-determining step involving breaking of the C–H bond of the surface $^*\text{CH}_3\text{O}$ intermediate [37]. The reactivity of the surface group VI metal oxide additives is almost negligible for formation of redox products, and the kinetics of the supported $\text{V}_2\text{O}_5/\text{Al}_2\text{O}_3$ catalysts, as well as of supported $\text{V}_2\text{O}_5/\text{TiO}_2$ [15] and $\text{V}_2\text{O}_5/\text{Nb}_2\text{O}_5$ [38], are independent of the presence of the surface modifiers. However, propane ODH over reducible metal oxides proceeds via activation of the C–H bond from the central carbon during adsorption, which also constitutes the rate-determining step [39]. The kinetic analysis suggests that the propane equilibrium adsorption constant is enhanced when the secondary surface metal oxide additives are present for supported $\text{V}_2\text{O}_5/\text{Al}_2\text{O}_3$ catalysts. Consequently, the secondary surface metal oxide additives are able to weakly adsorb propane in a precursor state and supply the weakly adsorbed propane to the active surface VO_x sites for propane ODH to propylene. This is shown schematically in Fig. 5, where propane also weakly adsorbs on the surface modifiers, which can supply the adsorbed propane to the active surface vanadia site for activation to propylene (shown as dotted lines). For the surface chromia modifier, an additional arrow originates from the surface M_xO_y species to propylene, arising from its intrinsic high activity (not shown for simplicity). Thus, the reaction-specific promotional effect of the secondary group VI surface metal oxide additives for propane ODH is a consequence of the presence of weakly chemisorbed propane on these relatively inert metal oxide sites that supply the propane to catalytic active redox site for activation to propylene. Furthermore, the current study demonstrates that the reactivity of the same surface metal oxide catalytic active sites, as well as their kinetic interactions,

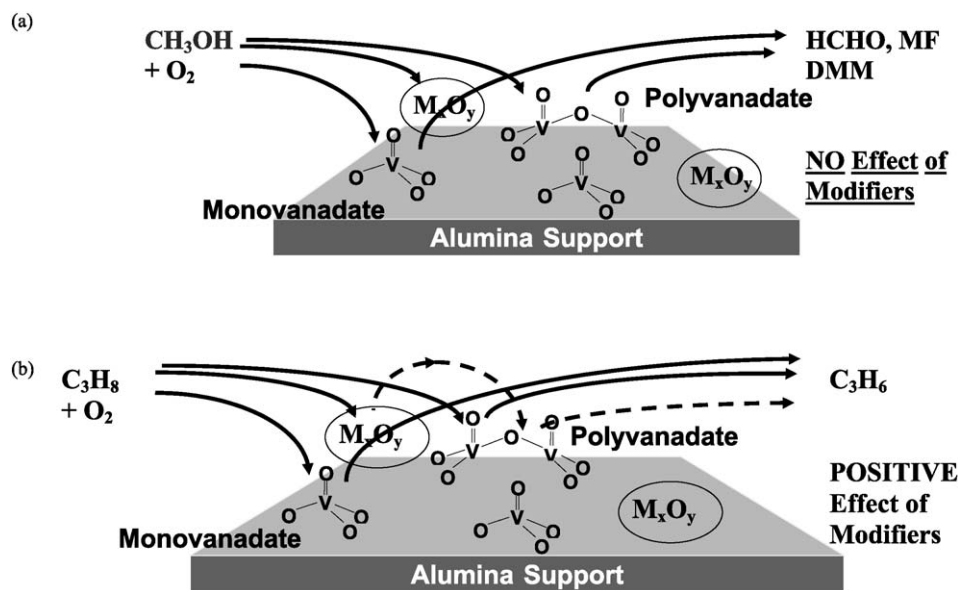


Fig. 5. Model of the (a) methanol oxidation reaction and (b) propane ODH reaction showing the effect of the secondary metal oxide additives, M_xO_y , on supported vanadia–alumina catalysts. For the surface chromia modifier, an additional arrow originates from the surface M_xO_y species to propylene and is not shown for simplicity.

is strongly dependent on the specific chemical probe molecules being used (H_2 , CH_3OH , and C_3H_8).

4. Conclusions

Supported vanadia–alumina catalysts were modified with secondary group VI (Cr, Mo, and W) metal oxide additives. Raman spectroscopy revealed that the metal oxide additives were present as surface MO_x species and that they did not form crystalline Cr–V–O, Mo–V–O, or W–V–O mixed-oxide phases. Raman spectroscopy and H_2 -TPR studies also demonstrated that the secondary surface metal oxides behaved as noninteracting additives that did not significantly alter the molecular structure of the surface VO_x species. The secondary surface metal oxide additives were relatively inert for methanol ODH under the chosen reaction conditions, and did not perturb the redox activity of the alumina-supported vanadia sites. However, during propane ODH to propylene, a significant promotional effect was seen due to the presence of the secondary surface metal oxide additives. The promotional effect is reflected in an enhanced kinetic pre-exponential factor associated with the propane equilibrium adsorption constant. It appears that the relatively inert secondary surface metal oxide additives (MoO_x and WO_x) are able to weakly adsorb propane in a precursor state that supplies the catalytic active VO_x sites for propane activation to propylene. Unlike the relatively inert surface WO_x and MoO_x modifiers, the surface CrO_x modifier has greater intrinsic activity for propane activation than the surface VO_x sites. Consequently, the enhanced activity of the alumina-supported CrO_x – VO_x catalyst is related to the partial supply of weakly adsorbed propane from the somewhat less active surface VO_x sites to the more active surface CrO_x sites. However, the selectivity of the propane to propylene reaction is lower over the surface CrO_x sites than over the surface VO_x sites.

Acknowledgments

G.D. gratefully acknowledges support from the Ministry of Human Resources (MHRD), India. I.E.W. gratefully acknowledges financial support from the Department of Energy-Basic Energy Sciences (grant DE-FG02-93ER14350). The authors thank T.V. Malleswara Rao, IIT Kanpur, for providing the Al_2O_3 reactivity data.

References

- [1] E.A. Mamedov, V. Cortés Corberán, Appl. Catal. A 127 (1995) 1.
- [2] T. Blasco, J.M. López Nieto, Appl. Catal. A 157 (1997) 117.
- [3] A. Khodakov, B. Olthof, A.T. Bell, E. Iglesia, J. Catal. 181 (1999) 205.
- [4] A.A. Lemonidou, L. Nalbandian, I.A. Vasalos, Catal. Today 61 (2000) 333.
- [5] G. Martra, F. Arena, S. Coluccia, F. Frusteri, A. Parmaliana, Catal. Today 63 (2000) 197.
- [6] X. Gao, J.-M. Jehng, I.E. Wachs, J. Catal. 209 (2002) 43.
- [7] N. Ballarini, F. Cavani, A. Cericola, C. Cortelli, M. Ferrari, F. Trifirò, G. Capannelli, A. Comite, R. Catani, U. Cornaro, Catal. Today 91 (2004) 99.
- [8] C.L. Pieck, M.A. Bañares, J.L.G. Fierro, J. Catal. 224 (2004) 1.
- [9] K. Routray, K.R.S.K. Reddy, G. Deo, Appl. Catal. A 265 (2004) 103.
- [10] E. Heracleous, M. Machli, A.A. Lemonidou, I.A. Vasalos, J. Mol. Catal. A 232 (2005) 29.
- [11] I.E. Wachs, Catal. Today 100 (2005) 79.
- [12] K. Routray, G. Deo, AIChE J. 51 (2005) 1733.
- [13] R.P. Singh, M.A. Bañares, G. Deo, J. Catal. 233 (2005) 388.
- [14] H. Dai, A.T. Bell, E. Iglesia, J. Catal. 221 (2004) 491.
- [15] G. Deo, I.E. Wachs, J. Catal. 146 (1994) 335.
- [16] M.A. Vuurman, D.J. Stufkens, A. Oskam, G. Deo, I.E. Wachs, J. Chem. Soc., Faraday Trans. 92 (1996) 3259.
- [17] M. Cherian, R. Gupta, M.S. Rao, G. Deo, Catal. Lett. 86 (2003) 179.
- [18] M.A. Bañares, S.J. Khatib, Catal. Today 96 (2004) 251.
- [19] S.W. Yang, E. Iglesia, A.T. Bell, J. Phys. Chem. B 109 (2005) 8987.
- [20] B. Grzybowska, J. Słoczyński, R. Grabowski, K. Samson, I. Gressel, K. Wciłso, L. Gengembre, Y. Barbaux, Appl. Catal. A 230 (2002) 1.
- [21] G.G. Cortez, J.L.G. Fierro, M.A. Bañares, Catal. Today 78 (2003) 219.

- [22] J.M. Lopez Nieto, R. Coenraads, A. Dejoz, M.I. Vasquez, in: R.K. Grasselli, S.T. Oyama, A.M. Gaffney, J.E. Lyons (Eds.), Proc. 3rd World Congress on Oxidation Catalysis, S. Diego, 1997, Elsevier, Amsterdam, 1997, p. 443.
- [23] V. Ermini, E. Finocchio, S. Sechi, G. Busca, S. Rossini, Appl. Catal. A 198 (2000) 67.
- [24] C. Resini, M. Panizza, L. Arrighi, S. Sechi, G. Busca, R. Miglio, S. Rossini, Chem. Eng. J. 89 (2002) 75.
- [25] X. Gao, Q. Xin, X. Guo, Appl. Catal. A 114 (1994) 197.
- [26] M. Machli, E. Heracleous, A.A. Lemonidou, Appl. Catal. A 236 (2002) 23.
- [27] I.E. Wachs, G. Deo, M.A. Vuurman, H. Hu, D.S. Kim, J.-M. Jehng, J. Mol. Catal. 82 (1993) 443.
- [28] A.M. Turek, I.E. Wachs, E. DeCanio, J. Phys. Chem. 96 (1992) 5000.
- [29] M.A. Bañares, I.E. Wachs, J. Raman Spectrosc. 33 (2002) 359.
- [30] A. Jones, B. McNicols, Temperature Programmed Reduction for Solid Materials Characterization, Marcel Dekker, New York, 1986.
- [31] M. Badlani, I.E. Wachs, Catal. Lett. 75 (2001) 137.
- [32] G. Deo, I.E. Wachs, J. Catal. 146 (1994) 325.
- [33] I.E. Wachs, Catal. Today 27 (1996) 437.
- [34] M.A. Vuurman, I.E. Wachs, J. Phys. Chem. 96 (1992) 5008.
- [35] M.A. Vuurman, I.E. Wachs, D.J. Stufkens, A. Oskam, J. Mol. Catal. 77 (1992) 263.
- [36] I.E. Wachs, C.C. Chersich, J.H. Iiardenbergh, Appl. Catal. 13 (1985) 335.
- [37] L.J. Burcham, M. Badlani, I.E. Wachs, J. Catal. 203 (2001) 104.
- [38] I.E. Wachs, J.-M. Jehng, W. Ueda, J. Phys. Chem. B 109 (2005) 2275.
- [39] G. Deo, M. Cherian, T.V.M. Rao, in: J.L. G Fierro (Ed.), Metal Oxides: Chemistry and Applications, CRC Press, Boca Raton, FL, 2006, p. 491.